

## PULSATIONS IN THE ULTRAVIOLET AND X-RAY SPECTRA OF VELA X-1

BRAM BOROSON AND RICHARD MCCRAY

JILA, Campus Box 440, University of Colorado, Boulder, CO 80309; boroson@jila02.colorado.edu, dick@jila.colorado.edu

TIMOTHY KALLMAN

Goddard Space Flight Center, Greenbelt, MD 20771; tim@xstar.gsfc.nasa.gov

AND

FUMIAKI NAGASE

Institute of Space and Astronautical Science, 3-1-1, Yoshinodai, Sagami-hara, Kanagawa 229, Japan

Received 1992 July 13; accepted 1996 January 22

### ABSTRACT

In simultaneous observations with the Faint Object Spectrograph aboard the *Hubble Space Telescope* and the large-area counters aboard *Ginga*, we obtained time-resolved ultraviolet and X-ray spectra of the X-ray binary HD 77581/4U 0900 – 40 (Vela X-1) during inferior conjunction of the X-ray source. We detected pulsations at the 283.33 s X-ray pulse period in the absorption lines Si iv  $\lambda$ 1402 and N v  $\lambda$ 1238, 1242. The pulse amplitudes in the UV lines were  $\sim 3\%$ . The profile of the pulsed UV intensity in the Si iv absorption line resembled that of the soft X-rays, while that in the N v line was anticorrelated with the profile of the hard X-ray pulsations. The effect is probably due to photoionization of Si iv and N iv in the stellar wind of HD 77581 by the rotating beam of Vela X-1.

*Subject headings:* stars: individual (Vela X-1) — stars: oscillations — X-rays: stars

### 1. INTRODUCTION

Although we understand that stellar winds from OB stars are accelerated by the transfer of momentum from stellar ultraviolet continuum photons to ions in the wind through resonance scattering, many uncertainties remain in the theory. For example, the theory does not account for the detailed shapes of the UV line profiles as a function of stellar spectral type. Moreover, the “superionization” of trace elements observed in the winds lacks a detailed accounting (Olson & Castor 1981). Evidently, instabilities in the radiative acceleration mechanism may lead to shocks in the wind that emit soft X-rays (Cassinelli & Olson 1979; Owocki & Rybicki 1984).

Several known X-ray binaries have massive OB companion stars with strong stellar winds. Indeed, in such systems gravitational capture of the stellar wind may contribute significantly to the accretion flow that powers the X-ray emission. The X-ray source in turn can modify substantially the dynamics of a stellar wind, by photoionizing trace elements in the wind and also through its gravity. Thus, observations of such systems may give us a new probe of the dynamics of stellar winds in general and of the accretion flows in particular.

Hatchett & McCray (1977) predicted that an X-ray source in such a system could photoionize trace elements in the wind. This would result in “bleached zones” devoid of the ions that create the P Cygni lines seen in the ultraviolet spectra of stars with strong stellar winds. The resulting variation of the P Cygni profiles with orbital phase was observed by the *International Ultraviolet Explorer* (IUE) satellite in several X-ray binaries, including Vela X-1 (Dupree et al. 1980). McCray et al. (1984, hereafter Paper I) then presented a model for the P Cygni line variability in this system, which consists of a neutron star orbiting a B 0.5 Ia supergiant with an 8.96 day period.

Kallman, McCray, & Voit (1987, Paper II) recognized that the timescales for the relevant ions in the wind of Vela X-1 to adjust their abundances to variations in the X-ray

illumination should be much less than the 283.33 s X-ray pulse period. They predicted that pulsations would be seen in the P Cygni profiles, but they failed to find such an effect in the C iv  $\lambda$ 1548, 1551 doublet in an observation with IUE.

On 1991 August 19, we detected pulsations in the UV P Cygni lines of Vela X-1 in observations taken with the Faint Object Spectrograph (FOS; Ford 1985) aboard the *Hubble Space Telescope*. Simultaneous observations taken with the *Ginga* X-ray telescope (Makino 1987) enabled us to correlate the UV pulsations with the X-ray pulsations. Here we report these results and discuss their implications.

### 2. OBSERVATION AND DATA ANALYSIS

#### 2.1. X-Ray Observations

*Ginga* observed Vela X-1 from 1991 August 18, 04:05 UT, to August 19, 19:20 UT, corresponding to X-ray orbital phases  $\phi_x = 0.34$ –0.53 (where  $\phi_x = 0$  at the midpoint of the eclipse of the X-ray source, and the ephemeris can be found from Deeter et al. 1987 and van der Klis & Bonnet-Bidaud 1984).

Data were read out in 0.5, 4, or 16 s intervals. Because of Earth occultations and the South Atlantic Anomaly, the net observation time is about one-third of the observation interval. The signal from *Ginga* during the time of the *HST* observations is shown in Figure 1.

Before the *HST* observation began, the X-ray luminosity emerged from a low state that had probably resulted from absorption by dense gas with column density  $N \gg 10^{24}$  cm $^{-2}$ . The average 2–37 keV X-ray luminosity rose from  $L_x \approx 3 \times 10^{36}$  ergs s $^{-1}$  during the first orbit of the *HST* observations to  $L_x \approx 4 \times 10^{36}$  ergs s $^{-1}$  during the second orbit, assuming a distance  $D = 2.0$  kpc (Sadakane et al. 1985). Fits to the X-ray spectra during the first and second *HST* orbits (Fig. 2) give absorbing column densities of  $1.8 \times 10^{23}$  and  $1.2 \times 10^{23}$  cm $^{-2}$ , respectively (assuming cosmic abundances), substantially greater than the column density  $\sim 5 \times 10^{22}$  cm $^{-2}$  typically seen by *Tenma* at this

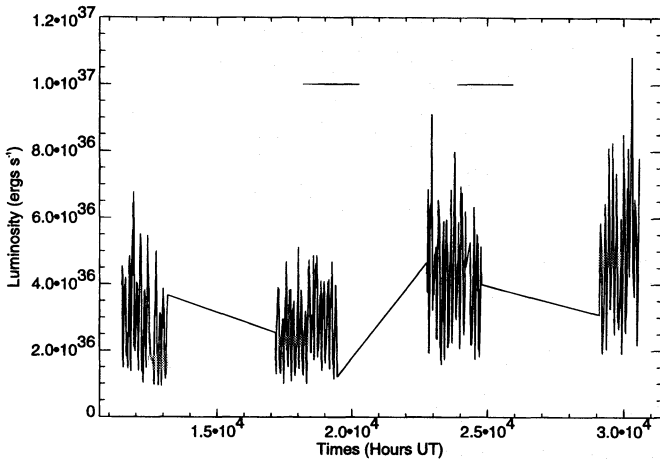


FIG. 1.—*Ginga* observations of 2–37 keV luminosity of Vela X-1 during the time of overlap with *HST* observations. A distance of 2.0 kpc was assumed. The horizontal lines indicate the times of the *HST* observations.

orbital phase (Sato et al. 1986). The fits also show a soft X-ray excess. This may result from an additional source of soft X-rays in the wind, such as the X-ray lines seen by *ASCA* (Nagase et al. 1994). However, another model (such as partial covering of the X-ray source by a clumpy absorber; Nagase et al. 1986) may be required to explain the pulsation of the soft excess during our observations.

The observed 283.33 s X-ray pulse period is consistent with the *Ginga* observation of 1988 February (Nagase 1989) and the spin-down rate since 1979. The pulse profiles have the same strong spectral dependence seen in *Tenma* observations (Nagase 1989). Figure 2 shows the time-averaged X-ray spectrum.

2.2. *HST* Observations

We observed Vela X-1 with the FOS on 1991 August 19, from 5:03 to 7:13 UT, corresponding to  $\phi_x = 0.459$  to  $\phi_x = 0.470$ . Two spacecraft orbits, interrupted by one Earth occultation, provided 71 minutes of data. The FOS in RAPID mode recorded counts every 19.5 s. We used the G130H grating with the 1" aperture, a configuration with

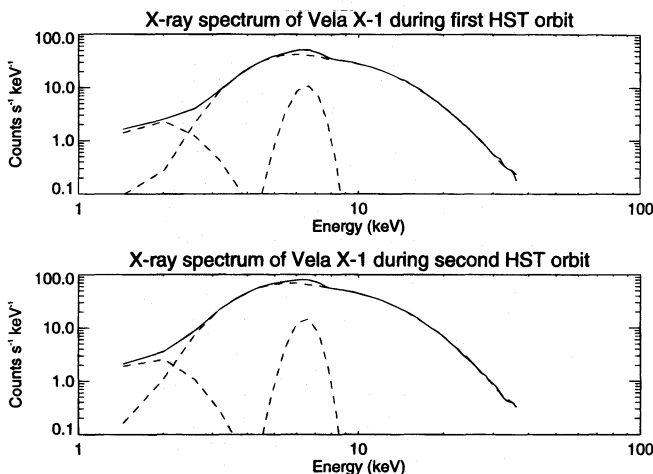


FIG. 2.—Time-averaged X-ray spectrum of Vela X-1 observed by *Ginga* during the two *HST* orbits on 1991 August 19. The dashed curves show the following components of fits to the spectra: a high-energy power law with absorption by cold gas of cosmic abundance; a 6.4 keV Fe K $\alpha$  fluorescence line; and a soft thermal bremsstrahlung component.

1.2 Å resolution, a range 1200–1600 Å, and a dispersion of 0.25 Å pixel<sup>-1</sup>.

The time-averaged UV spectrum (Fig. 3) is consistent with that observed by *IUE* (Dupree et al. 1980). The P Cygni lines of C iv  $\lambda\lambda$ 1548.19, 1550.76, Si iv  $\lambda\lambda$ 1393.75, 1402.77, and N v  $\lambda\lambda$ 1238.81, 1242.80 are clearly visible. In addition, several narrow interstellar lines are evident.

The average flux in the deepest parts of the Si iv absorption doublet was about 20% greater during the second *HST* orbit than during the first (Fig. 4), evidently because of increasing photoionization of Si iv in the stellar wind by the X-ray source. The apparent change in the red P Cygni emission is probably the result of a decrease of the continuum flux by 1%–2% between the two *HST* orbits.

To search for pulsations in the UV spectrum, we used the phase dispersion minimization (PDM) method (Stellingwerf 1978; Davies 1990). First, to improve counting statistics, for each wavelength we summed the counts over a range of 20 adjacent pixels, i.e., spanning a range of 5 Å (the results did not depend greatly on the wavelength range chosen). Then, for a given trial pulsation period we divided the data into

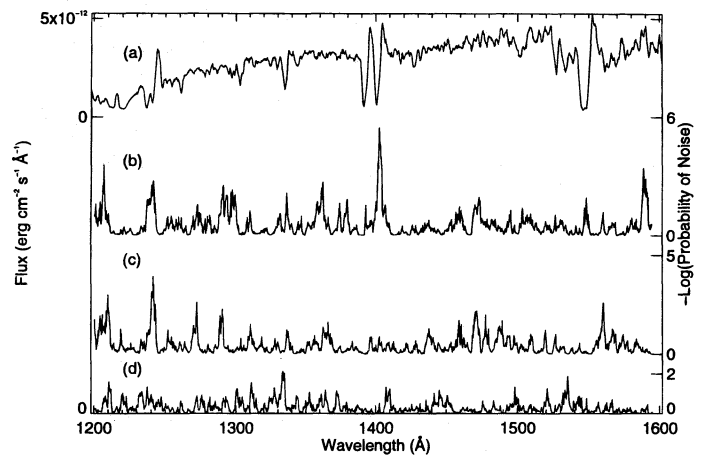


FIG. 3.—The result of a search for pulsations in the UV spectrum of Vela X-1. Curve *a* shows the time-averaged spectrum; curves *b*, *c*, and *d* show the probability of no pulsation in the flux of 5 Å bins centered on each wavelength, for test periods of 283.33, 283.33/2, and 180 s, respectively.

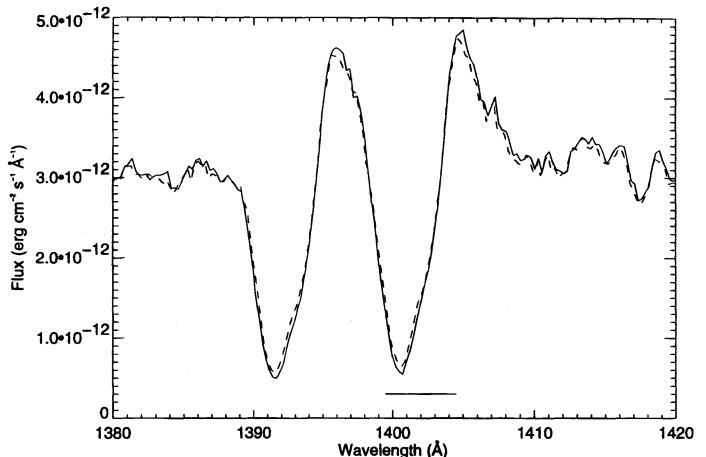


FIG. 4.—The profiles of Si iv during the first (solid line) and second (dashed line) *HST* orbits. The horizontal line shows the wavelength range in which pulsations were found.

six pulse-phase bins and summed the flux in each phase bin. The counting statistics were very good; for example, in a 5 Å range centered at 1402 Å (in the Si iv absorption line), we had  $N \sim 4 \times 10^4$  net counts per phase bin, giving  $N^{-1/2} \sim 0.5\%$ . We applied standard analysis of variance methods to compare the variance within these time bins to the variance in the overall data. This gives a statistic  $L$  from which we can calculate the probability  $P(L)$  that the data do not pulse at the trial period (Davies 1990).

Figure 3 displays the results. Searching for pulsations at the 283.33 s X-ray pulse period, we see a very significant peak [probability  $P(L) \sim 10^{-6}$  for random occurrence] centered at 1402 Å, in the red component of the Si iv absorption doublet. The next most significant signals [ $P(L) \sim 10^{-4}$ ] are centered at 1205 and 1590 Å, wavelengths that do not correspond to any observed spectral features. There is also a peak [ $P(L) \sim 10^{-3}$ ] centered at 1241 Å. This peak is probably significant because it is in the N v absorption line, where we have an a priori expectation of finding pulsations. The other peaks with  $P(L) \sim 10^{-2}$  to  $10^{-3}$  are not particularly significant, since they do not correspond to any spectral feature and we are scanning  $\sim 500$  independent wavelength bands. A hint of pulsation shows up in the C iv  $\lambda\lambda 1550$  absorption line, but the statistical significance is not great. Nor is pulsation detected in the blue component of Si iv  $\lambda\lambda 1394, 1403$ .

When we search for pulsation at 283.33/2 s (Fig. 3), we see a clear signal [ $P(L) \sim 10^{-5}$ ] at 1241 Å in the N v absorption line and no signal of comparable significance at any other wavelength.

Testing for pulsations at many other trial periods, we found no peaks with significance comparable to the detections at 283.33 s in Si iv  $\lambda 1402$  and at 283.33/2 s in N v  $\lambda 1241$ . A typical example is shown in Figure 3.

In the method described above, we scanned wavelength to search for pulsations at a specified period. Alternatively, one can specify the wavelength range and scan through frequency by constructing a power spectrum. When we do so for the 5 Å band centered at 1402 Å, we see a peak at a period 283.33 s and no comparable peaks at any other period. Likewise, for the 5 Å band centered at 1241 Å, we see a strong peak at 283.33/2 s, a weaker peak at 283.33 s, and no comparable peaks at any other period. The peaks in the power spectra have considerable sideband structure due to the observation and readout schedules. This structure vanishes when we employ a CLEAN algorithm (Roberts, Lehar, & Dreher 1987) kindly provided by R. White.

By these methods we searched for evidence of pulsation in a two-dimensional parameter space ( $\lambda, P$ ) of wavelength and pulse period. We scanned a good fraction of this space and found no signals of comparable significance to the ones at (1402.0 Å, 283.33 s) and (1241 Å, 283.33/2 s). Thus, we have no doubt that the pulsations are real.

### 2.3. Pulse Amplitudes and Profiles

Figures 5a–5d illustrate the pulse profiles of the X-ray and UV signals. The X-ray signal is strongly pulsed, with amplitudes  $\sim 45\%$  in the 1.2–2.3 keV band (Fig. 5a) and  $\sim 55\%$  in the 13.5–18.5 keV band (Fig. 5b) of the time-averaged signal. In contrast, the pulsations in the Si iv

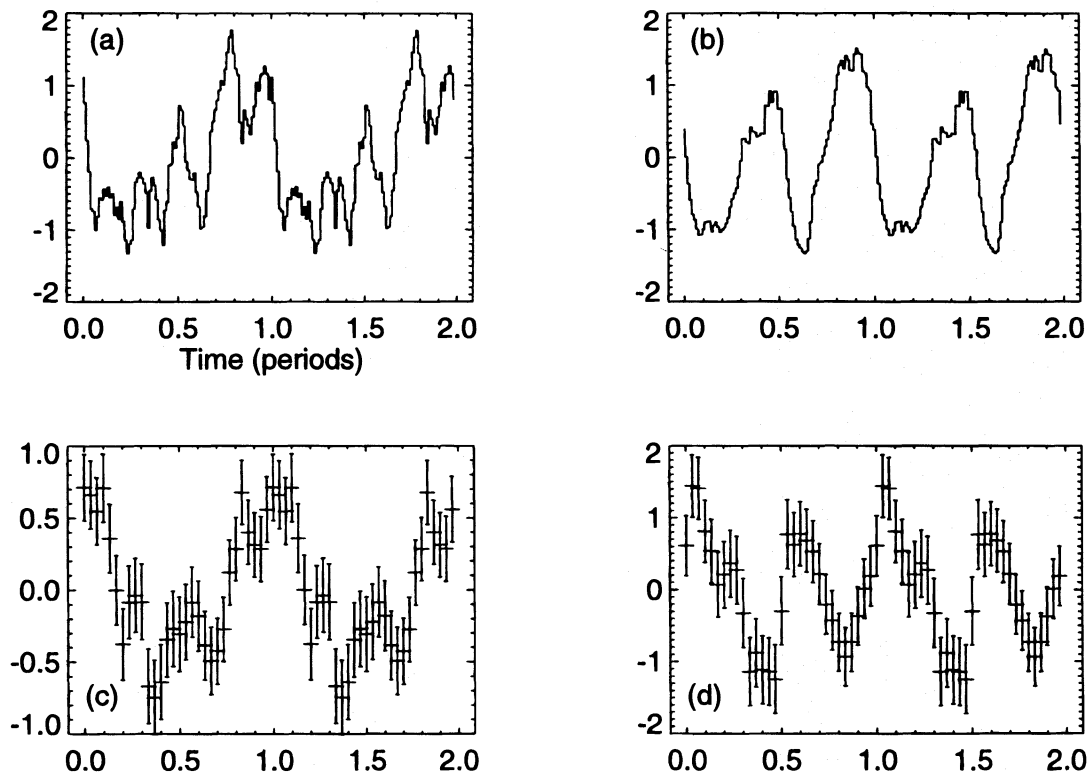


FIG. 5.—X-ray and UV pulse profiles. (a) 1.2–2.3 keV X-ray pulse profile; (b) 13.5–18.5 keV X-ray pulse profile; (c) pulse profile of the UV intensity in the Si iv absorption line (1400–1404 Å); and (d) pulse profile in the N v absorption line (1238.5–1243.5 Å). For each, two full pulse periods are shown. Amplitude 1.0 corresponds to (a) 30%, (b) 40%, (c) 3%, and (d) 3% of the time-averaged signal in the respective bands. Error bars for the UV profiles correspond to  $1\sigma$  counting statistics.

$\lambda 1402$  and N v  $\lambda 1241$  lines have amplitudes of 2.3% and 4%, respectively.

The X-ray pulse profile changes from the 1.3–2.3 keV profile (Fig. 5a) to the nearly symmetrical double-pulse shape (Fig. 5b) at  $\sim 13$  keV. The UV pulse profiles differ markedly from each other. The Si iv profile (Fig. 5c) resembles the 1.2–2.3 keV X-ray pulse profile (Fig. 5a); the intensity in the Si iv absorption *increases* with increasing X-ray intensity, and the pulse profiles agree best if the UV pulsations are delayed  $\sim 15$  s with respect to the X-ray pulsations. The N v profile (Fig. 5d) has a double pulse shape that closely resembles the negative of the hard X-ray profile (Fig. 5b), i.e., the intensity in the N v absorption line *decreases* with increasing hard X-ray intensity. The N v pulse profile is shifted by less than 10 s from the negative of the hard X-ray pulse.

### 3. DISCUSSION

#### 3.1. Effects of the Binary Orbit on P Cygni Lines

The time-averaged spectrum observed by the FOS disagrees with the predictions of Paper I for the P Cygni profiles at inferior conjunction of the X-ray source. Paper I predicted that the X-rays would ionize most of the Si iv on the near side of the wind, but the FOS found deep Si iv  $\lambda 1394, 1403$  absorption. (Dupree et al. 1980 found a similar result with *IUE*.) The C iv absorption is also deeper than expected.

If the large column density of absorbing material found in the *Ginga* observation ( $\sim 5$ – $10$  times that assumed in Paper I) results from material near the source that covers a large solid angle, the soft X-rays will not illuminate the wind at large distances. McCray et al. (1984) showed that the populations of Si iv and C iv are very sensitive to the flux at 50 eV–1 keV that cannot be observed directly owing to the absorption by the stellar wind and interstellar gas (Daltabuit & Meyer 1972). With the high observed absorption, we can expect the X-ray source to be much less effective in removing these ions.

#### 3.2. Pulsations in P Cygni Lines

Kallman et al. (1987) predicted that the C iv line would pulse with an amplitude of  $\sim 30\%$  of the total flux. Instead, pulsations were detected only in the Si iv  $\lambda 1402$  and N v  $\lambda 1241$  lines, and at only  $\sim 3\%$  of their total flux. We found pulsations in only the red component of the Si iv doublet. This result is reasonable: the blue component, with twice the oscillator strength, is more saturated. As can be seen from Paper I, X-rays ionize Si iv more efficiently than C iv, explaining our failure to detect pulsations in the C iv line.

The lack of detailed agreement between the predictions of Paper II and the results of the *Ginga*/FOS observation is not surprising. If X-rays do not penetrate very far into the dense gas, the “bleached zones” will be small. In addition, Kallman et al. made a number of simplifications in order to show that P Cygni pulsations were possible. For example, they assumed that the neutron star rotation axis was parallel to the axis of the binary orbit and that the X-ray beam was independent of latitude (a fan beam). The observed X-ray pulse profile shows only that part of the X-ray beam that cuts through the observer’s line of sight. In contrast, the UV absorption-line profiles reflect the ionization of atoms in the entire tube subtending the stellar disk, which is illuminated by a large range of X-ray beam latitudes. Given

the soft X-ray excess and the observed variability of the soft X-ray absorption, it would not be surprising if the wind in this tube was illuminated by quite a different ionizing beam than the one we infer from the X-ray pulse profile.

Moreover, Kallman et al. (1987) also assumed that recombination photons of Si v (ionization energy 45.1 eV) and C v (64.5 eV) escape freely, while in fact they may diffuse out of the wind slowly owing to substantial optical depths in the He II Balmer and Lyman continua (Masai 1984). This effect would couple the ionization in different parts of the wind at different times, requiring a more sophisticated model than that of Paper II.

In contrast to Si iv and C iv, X-ray ionization should *increase* the amount of N v in most of the wind, where N iv is expected to be the dominant ionization stage in the absence of X-ray illumination. On this basis Kallman et al. predicted an anticorrelation between N v absorption and X-ray illumination, which we have now observed with the FOS.

#### 3.3. Delays and Doppler Shifts

The apparent delay between pulsations in X-rays and in the Si iv  $\lambda 1403$  line is short ( $\approx 15$  s). This result suggests that the region of the wind most responsible for the pulsation is probably near the pulsar and along the line of sight. Yet most of the pulsation is seen in the wavelength range  $1400 \text{ \AA} < \lambda < 1404 \text{ \AA}$ . That is, we found pulsations near the rest wavelength ( $1402.77 \text{ \AA}$ ) of the red component of the Si iv doublet, in a region overlapping both P Cygni absorption and emission (see Fig. 4). Observations during eclipse suggest that the undisturbed wind velocity should be  $\approx 500 \text{ km s}^{-1}$  near the neutron star. For the Si iv component at  $1403 \text{ \AA}$ , we would then expect to see the pulsation at  $\approx 1400 \text{ \AA}$ . Perhaps the radial wind velocity near the neutron star has been reduced by hydrodynamic effects such as those described by Blondin et al. (1990).

If the UV pulsations arose in the region between the neutron star and the primary, it would be hard to explain the similarity between X-ray and P Cygni line pulse shapes. The neutron star would have to rotate  $180^\circ$  for the beam to reach this region, and we would expect a delay between X-ray and UV peaks of  $\sim 283/2$  s. The similarity between X-ray and Si iv  $\lambda 1402$  pulsations further suggests that the X-ray beam shape does not vary rapidly with latitude.

#### 3.4. Future Work

Studies of rapid variability of UV lines in X-ray binaries promise to tell us much about the nature of accretion flows. We expect the phase lags between X-ray and UV pulsations to vary substantially with orbital phase; observing this change will enable us to map the shape of the X-ray beam and the dynamics of the wind more thoroughly. If there is less soft X-ray absorption during another observation, the P Cygni lines may pulse more strongly.

On 1993 November 21 we revisited Vela X-1 with the FOS in RAPID mode. However, because of a target acquisition failure, the count rate was a tenth of that expected, and we were unable to detect any pulsations. The unidentified UV spectral lines persisted, and are a good topic for further research.

Similar observations may prove successful in other massive X-ray binary systems. The orbital effect predicted by Hatchett & McCray (1977) has been seen in Cygnus X-1 (Treves et al. 1980), LMC X-4 and SMC X-1

(Hammerschlag-Hensberge 1980), and 4U 1700 – 37/HD 153919 (Hammerschlag-Hensberge, Kallman, & Howarth 1984). In systems without an X-ray pulsar, rapid variability in X-rays may be reflected in the UV lines. Simultaneous X-ray/UV observations may allow us to model the winds of these systems.

This work is based on observations with the NASA/ESA *Hubble Space Telescope*, obtained at the Space Telescope Science Institute, which is operated by the Association of

Universities for Research in Astronomy, Inc., under NASA contract NAS 5-26555. We thank John Castor, Rick White, Ron Wurtz, and Anne Kinney for their advice and assistance. The *Ginga* satellite entered the atmosphere 2 months after these observations were made. We would not have been able to obtain these results without an extraordinary response to this exigency by Lauretta Nagel and her colleagues at the User Support Branch of the Space Telescope Science Institute. We thank Yasuo Tanaka for helping to arrange and support our collaboration.

## REFERENCES

- Blondin, J. M., Kallman, T. R., Fryxell, B. A., & Taam, R. E. 1990, *ApJ*, 365, 591  
 Cassinelli, J. P., & Olson, G. L. 1979, *ApJ*, 229, 304  
 Daltabuit, E., & Meyer, S. 1972, *A&A*, 20, 415  
 Davies, S. R. 1990, *MNRAS*, 244, 93  
 Deeter, J., Boynton, P., Shibasaki, N., Hayakawa, S. F., & Sato, N. 1987, *AJ*, 93, 877  
 Dupree, A. K., et al. 1980, *ApJ*, 238, 969  
 Ford, H. C. 1985, *Faint Object Spectrograph Instrument Handbook* (Baltimore: STScI)  
 Hammerschlag-Hensberge, G. 1980, in *Proc. Second IUE Conf.* (ESA SP-157), lix  
 Hammerschlag-Hensberge, G., Kallman, T., & Howarth, I. 1984, *ApJ*, 283, 249  
 Hatchett, S., & McCray, R. 1977, *ApJ*, 211, 552  
 Kallman, T. R., McCray, R., & Voit, G. M. 1987, *ApJ*, 317, 746 (Paper II)  
 Makino, F. 1987, *Astrophys. Lett. Commun.*, 25, 223  
 Masai, K. 1984, *Ap&SS*, 106, 391  
 McCray, R., Kallman, T. R., Castor, J. I., & Olson, G. L. 1984, *ApJ*, 282, 245 (Paper I)  
 Nagase, F., Hayakawa, S., Sato, N., Masai, K., & Inoue, H. 1986, *PASJ*, 38, 547  
 Nagase, F. 1989, *PASJ*, 41, 1  
 Nagase, F., Zylstra, G., Sonobe, T., Kotani, T., & Inoue, H. 1994, *ApJ*, 436, L1  
 Olson, G. L., & Castor, J. I. 1981, *ApJ*, 244, 179  
 Owocki, S. P., & Rybicki, G. B. 1984, *ApJ*, 284, 337  
 Roberts, D. H., Lehar, J., & Dreher, W. 1987, *AJ*, 83, 968  
 Sadakane, K., et al. 1985, *ApJ*, 288, 284  
 Sato, N., et al. 1986, *PASJ*, 38, 731  
 Stellingwerf, R. F. 1978, *ApJ*, 224, 953  
 Treves, A., et al. 1980, *ApJ*, 242, 1114  
 van der Klis, M., & Bonnet-Bidaud, J. 1984, *A&A*, 135, 155